RSC Advances

PAPER

View Article Online
View Journal | View Issue

Cite this: *RSC Adv.*, 2017, **7**, 15284

The effects of dissociated rods and rod-surfaced microspheres on bone mesenchymal stem cellular viability†

Xiao Liu,‡[ab] Naru Zhao,‡[ab] Haibo Duan,[a] Yijuan Ma,[a] Xiaoheng Guo,[ab] Jingjing Diao,[ab] Xuetao Shi[ab] and Yingjun Wang*[ab]

Received 7th December 2016
Accepted 21st February 2017

DOI: 10.1039/c6ra27861b

rsc.li/rsc-advances

Material properties and cellular behaviours seemed to be coupled, implying the existence of reciprocities between cells and materials. Understanding cellular behaviours and material structure is indispensable for materials synthesis and design but has mostly focused on shape, neglecting the status of the sub-structure. Hence we utilized a similar route to regulate the different morphology of HAp particles and then investigated reciprocities between particles and bone marrow mesenchymal stem cells (BMSCs). Based on our cell experiment, we revealed the side effects of dissociated micro-rods on cellular behaviours. Despite the facts that both particles showed modestly cytotoxicity, the multi-structure HAp sphere could positively-regulate the proliferation, viability and differentiation of bone marrow mesenchymal stem cells (BMSCs) which indicated that the dissociated micro-rods may deteriorate the biological properties *in vitro*.

1. Introduction

Natural bone could be regarded as a mineralized matrix, a complex compound of biopolymer and biomineral.[1] Hydroxyapatite (HAp), whose chemical compositions are similar to the natural bone minerals,[2] possesses good biocompatibility, bioactivity and osteoconductivity. Based on these advantages, applications are diverse like bone filler, surface coating, prosthesis, carrier for drugs *etc.*[3] Numerous studies had been focusing on the morphology regulation of HAp granules and investigating the effect on cellular behaviours. In the present, various processing techniques were developed for the production of micro and nano HAp particles. For example, using the biocompatible inorganic substance like riboflavin-59-phosphate monosodium salt (RP) or DNA,[4,5] the self-assembly of biomolecule can not only regulate the structure but improve the biocompatibility simultaneously. Other template like biological template (yeast *etc.*[6]) and calcium carbonate (including pearl and some marine organism[7,8]) also exhibited a good application prospect.

Indeed, although many different morphologies and multi-hierarchical HAp have been synthesized, the conclusions of their interactions to cell were varied[9–13] or even contradictory[14–16] due to the different model parameter. Besides, much research has been focusing on hierarchical structure neglecting the status of sub-block unit whose status are the basic of physical or chemical properties. There still exists consensus widespread reached at present: the effect of HAp particles are size and dose dependent.[17] The common research studies reckoned microsphere HAp outweighs the micro-rod or needle-like HAp since microsphere HAp possess better cargo delivery ability,[18] multi-hierarchical structure, low cytotoxicity and promoting proliferation and differentiation.[19] Moreover, dissociated rod fixed in relative static flat could up-regulate the particle property because *in vivo* wear particles lead to HAp scaffold implant failure that monocyte secrete inflammatory factors.[14,16] The wear particles and dissociated micro-rod HAp may in a similar way to arouse the side effects.

In our study, sodium citrate were utilized as regulation agents.[20,21] Briefly, citrate can nucleate *via* aggregating with calcium ion under acid pH then crystal nucleus undergone fractal growth to form a sphere crystal. To assure the different shaped HAp shares similar physical–chemical properties, a novel and facile route was applied to synthesize different shape of HAp granules then investigating the biological performances. Moreover, some researchers have synthesized millimetre-level long HAp fiber *via* adding propanamide that would specific adsorption onto α, β plane leading to elongation along with c axis.[22] In this test, propanamide were utilized as co-regulation agent to obtain large-scale microsphere with 700 nm HAp rod block unit building surrounding it. We selected bone marrow mesenchymal stem cells as model cell, mBMSCs were co-cultured with the particles and their viability, proliferation, cytotoxicity and differentiation were investigated.

[a]*National Engineering Research Center for Tissue Restoration and Reconstruction, Guangzhou, China. E-mail: imwangyj@163.com*

[b]*School of Materials Science and Engineering, South China University of Technology, Guangzhou 510641, China. E-mail: nrzhao@scut.edu.cn; Tel: +86-20-87114645*

† Electronic supplementary information (ESI) available. See DOI: 10.1039/c6ra27861b

‡ The author contributed equally to the work.

2. Experimental section

Trisodium citrate (TSC), calcium nitrate (Ca-nitrate), ammonium phosphate ($(NH_4)_2HPO_4$) and nitric acid (HNO_3) were supplied from Guangzhou Chemical Reagent Factory (Guangdong, China). PA and ammonia hydroxide (NH_4OH) were purchased by Aladdin (Shanghai, China). All chemical reagents were of analytical grade without any further purification. Deionized water (DI-water) was obtained from a water purification system (Millipore S.A.S., France).

2.1 Synthesis of HAp multi-hierarchical microspheres

The synthesis process operated as our previous work.[23] Compendiously, stock solutions of Ca^{2+} and PO_4^{3-} were prepared respectively by dissolving Ca-nitrate and $(NH_4)_2HPO_4$ in a 0.2 M HNO_3 solution. The Ca/P molar ratios were 1.67. TSC were added to the Ca^{2+} while the PA were to PO_4^{3-} solutions. Then, the Ca^{2+} solution was added to the PO_4^{3-} solution under continuous stirring and the initial pH was adjusted to 3 with 2 M HNO_3. The reagent solutions were transferred to a Teflon-lined stainless steel autoclave. The autoclave was treated at the 180 °C for 24 h. The products were separated by centrifugation at a rate of 4000 rpm for 5 min, washed five times with deionizer water, freeze-drying and thermal treatment at 700 °C for 3 h to remove additions. These samples were designated as Multi-HS (multi-structure HAp sphere).

2.2 Synthesis of HAp sub-micro-rod

A similar treatment process utilized to synthesize HAp micro-rod,[19] a solution of diammonium phosphate ($(NH_4)_2HPO_4$, 12 mM, 60 ml) was vigorously stirred and the pH of the solution was adjusted to 4 with 2 M HNO_3. Then, Ca-nitrate (20 mM) was quickly added into the mixture under vigorous stirring. The pH of the mixture was further adjusted to 5 with 1 : 1 NH_4OH. 0.9 g sodium citrate was not added until the mixture was homogeneous. The reagent solutions were transferred to a Teflon-lined stainless steel autoclave. The autoclave was treated at the 180 °C for 2 h, later procedure were the same with the microsphere. These samples were designated as Disso-HR (dissociated HAp rod).

2.3 X-ray diffraction analysis

The mineralogical phase was analyzed by X-ray diffraction. X-ray diffraction measurements were performed on a PANalytical X'Pert PRO X-ray diffractometer *via* Cu Kα (λ = 0.15418 nm) incident radiation with the XRD data collected ranging from 10 to 60° in intervals of 0.02 at a scan rate of 1° per min.

2.4 Particle size, zeta potential and morphology determination

The size distribution was measured by DLS (Zetasizer Nano ZS, Malven Instruments, UK). The mean of the three measurements was recorded as the value and the zeta potential of the particle was also characterized by Zetasizer nano ZS. The morphology of the HAp particles was investigated by a field emission scanning electron microscope system (SEM, MERLIN compact, ZEISS, Germany).

2.5 Cell culture and seeding

Mouse bone mesenchymal stem cells (mBMSCs) purchased from ATCC (ATCC CRL-12424) were utilized and cultured in Dulbecco's Modified Eagle's Medium (DMEM, Gibco, USA) supplemented with 10% fetal bovine serum (FBS, Life Technologies, Gibco, USA) and 1% penicillin–streptomycin at incubator in a moist environment with 5% CO_2 and 37 °C. The medium was replenished at certain interval and trypsinization using 0.25% of trypsin–EDTA solution to collect the cells followed by subculture. mBMSCs around 4–6 passages were used in the following experiments. Cell suspensions (1 ml) were initially dropped onto the tissue culture plates subsequently cultured along for overnight, and then cocultured with materials. Based on our previous research,[19] cytotoxicity was sensitive to particle dose and 100 μg ml^{-1} was chose as materials seeding density which did not cause dose-induced cytotoxicity. Briefly, particles sterilized with autoclaving treatment and suspended with DMEM by ultrasonic before seeding. The same suspension density was prepared to insure the similar seeding rate, stabilities and dispersions in cell culture media. In addition, after settling the particles to the bottom, gently wobble the plate (crosswise instead of circle wobble) to disperse the materials.

As for cell differentiation measurement, the Dulbecco's Modified Eagle's Medium were mixed 10 mM b-glycerophosphate, 50 mM ascorbic acid, and 100 nM dexamethasone (all these reagents were purchased from Sigma). The osteogenesis induced reagent were not added until cell were cultured with DMEM for 2 days.

2.6 Cell proliferation and viability

Materials sterilized with autoclaving treatment were suspended with DMEM by ultrasonic to ensure a well-distributed suspension of HAp particles. Cell proliferation and viability was assessed by CCK-8 assay (Dojundo, Kumamoto, Japan) which is based on intra-cellular dehydrogenase viability and no harm to cell. For CCK-8 experiment, cell density is 1×10^4 per cm^2 and culture for 1, 3, 5 days in 24-well tissue culture polystyrene. When operating the measure, CCK-8 solution composed of 300 ml fresh culture medium and 30 ml CCK-8 stoste was added to each well; then 100 ml supernatant was transferred into a 96-well plate after the plate was incubated at incubator for 1 h, and the absorbance was analyzed with wavelength at 450 nm. Cell viability calculations are according to CCK-8 specification:

$$\text{Cell viability}(\%) = \frac{A_{\text{expriment group}} - A_{\text{blank}}}{A_{\text{positive control}} - A_{\text{blank}}}$$

A_{blank} represents the absorbance of reagent consist of only DMEM and CCK-8 solution while $A_{\text{positive control}}$ is cell mixed with DMEM and CCK-8 solution without materials.

2.7 Cytotoxicity of particles

Cytotoxicity was quantitatively assessed by LDH viability (Pierce LDH cytotoxicity Assay kit, thermo) which is based on detecting lactate dehydrogenase only released from damaged cell and maintained competence in DMEM. Procedure as follows: 100 μl supernatant from cell-materials coculture

system were transferred into 96-well plate then added the same volume LDH assay incubating at room temperature for 1 h before mixing the stop solution. The absorbance of the mixtures was measured at wavelength of 490 nm and 680 nm (Thermo 3001 Microplate Reader, USA) respectively. The determine LDH activity is subtracting 680 nm absorbance value from 490 absorbance value.

Live and Dead staining for qualitative analysis. To distinguish live cell from the dead, Live and Dead staining consist of the reagents with PI compound with DNA and calcein-AM. Fluorescence excitation to emit green and red fluorescence and then observed under fluorescence inversion microscope system.

2.8 Cell differentiation: real-time quantitative reverse transcription-polymerase chain reaction

mBMSCs at a cell density of 1×10^4 cells per cm^2 were cultured in DMEM with the materials for 2 days. Osteogenesis induced reagent were utilized to culture cell since then. TRIZOL, chloroform and isopropanol were used to cell lysis, RNA extraction and RNA precipitation respectively while TAKARA assay to reverse transcription to cDNA.[19] Specifically, the extracted RNA was isolated *via* Hipure Total RNA kits (Magentec, China) ($n = 4$) according to the manufacturer's protocol. Then the RNA were quantified by a NanoDrop2000 spectrophotometer (Thermo Scientific, USA) and normalized before reverse transcription. The RNA was reverse transcribed into cDNA using a PrimeScript RT reagent Kit with gDNA Eraser (TaKaRa Biotechnology, Japan).

The yielded complementary (cDNA) were performed with QuantStudio 6 flex RT-PCR system software (applied biosystems, USA), and examined the gene expression of housekeeping gene GAPDH, the alkaline phosphatase (ALP), the alpha 1 chain of type I collagen (Col-I), osteocalcin (OC), osteopontin (OPN) and osterix (OSX). Adopted primers sequences were listed in Table 1. The quantitative polymerase chain reaction (qPCR) was conducted with a SYBR green assay (Iq supremix, Bio-rad). The gene expressions were quantified with a calculation of $2^{\Delta\Delta C}$, where C represents the cycle times when the threshold was reached.

2.9 Protein secretion of mBMSCs

As an supplement to measurement cell differentiation, we investigated the secretion of osteogenic maker-alkaline phosphatase. ALP staining (BCIP/NBT purchased from KPL, USA) and ALP colorimetric kit (JIANCHENG, China) were used to investigate the alkaline phosphatase (ALP) secretion qualitatively and quantitatively. For ALP colorimetric kit, we utilized phenylmethylsulfonyl fluoride (PMSF) mixed with Radio-Immunoprecipitation Assay (RIPA) to lyse cells. Cell cultured for 7 days then measure ALP secretion.

Table 1 Validated primer sequences for RT-PCR

Gene	Direction	Sequence (5′–3′)
GAPDH	Forward	TGTGTCCGTCGTGGATCTGA
	Reverse	TTGCTGTTGAAGTCGCAGGAG
ALP	Forward	TGCCTACTTGTGTGGCGTGAA
	Reverse	TCACCCGAGTGGTAGTCACAATG
Col-I	Forward	ATGCCGCGACCTCAAGATG
	Reverse	TGAGGCACAGACGGCTGAGTA
OPN	Forward	TGCAAACACCGTTGTAACCAAAAGC
	Reverse	TGCAGTGGCCGTTTGCATTTCT
OCN	Forward	AGCAGCTTGGCCCAGACCTA
	Reverse	TAGCGCCGGAGTCTGTTCACTAC
OSX	Forward	CGTCCTCTCTGCTTGAGGAA
	Reverse	CTTGAGAAGGGAGCTGGGTA

2.10 The reciprocities of cell and particles

Via field emission scanning electron microscope system (SEM, MERLIN compact, ZEISS, Germany), we investigated the interacts between cell and particles. The cell and materials seeded on round coverslip and we operated an dehydration treatment to samples undergone fixation with 2.5% glutaraldehyde for more than 12 h before spraying Pt. The alcohol gradient dehydration treatment as follows: after washing twice with PBS to remove the glutaraldehyde, samples treated by 50%, 70%, 80%, 90%, 95% and 100% alcohol orderly, and the time were 60 min, 30 min, 20 min, 10 min, 5 min and 5 min successively. Then placed in a drying oven till alcohol vapored out.

2.11 Statistical analysis

Experiments results were expressed as means with standard deviations as error bar. CCK-8 assay, LDH assay and RT-PCR analysis results were evaluated by one way analysis of variance (ANOVA). Tukey's test with statistical significance set at $p < 0.05$ (marked as #) were used to analyze a comparison between two samples.

3. Results

3.1 Characterization of materials

The as-prepared samples were characterized with SEM and the morphology shown in Fig. 1. In the image, the prepared hierarchical structure microsphere (designated as Multi-HS) endowed with sub-micro rods as the block unit. Dissociated sub-micro-rods (designated as Disso-HR) were obtained *via* a similar synthetic process. Both of particles are uniform and the sub-micro rods located on Multi-HS as the block unit shared the same size with Disso-HR.

Size distribution and cumulative distribution of particles revealed that Disso-HR were more uniform with 700–800 nm in length. Moreover, the diameter of the Multi-HS were around 10 μm which was accordance with the SEM result. From the measurement results, the Multi-HS uniformity was inferior to Disso-HR with diameter from 9–12 μm which may caused by the block unit located on the surface. Additionally, the general size of Multi-HS ranging from 1 to 50 μm. Under ultrasonic oscillations before measurement, the block unit located on the Multi-HS break away from matrix arouse the inchoate size distribute column while the later distribute column maybe attributed to the aggregation phenomenon.

The XRD were utilized to characterize the mineralogical phase (Fig. 2). The XRD patterns indicated that no impurity phase were identified and the peaks, including the intensity and position, matched the hexagonal standard HAp perfectly (01-089-6438).

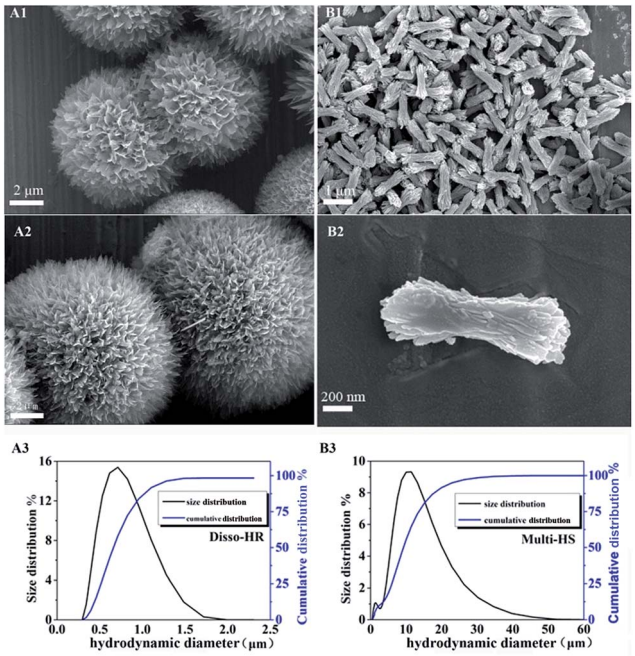

Fig. 1 SEM image of the particles. (A1 and A2) Hierarchical microsphere hydroxyapatite; (B1 and B2) micro-rod as control samples. (A3 and B3) Size distribution and cumulative distribution Disso-HR and Multi-HS respectively.

Besides, the similar XRD patterns indicated Multi-HS shared similar crystal phase and crystallinity with Disso-HR and insured similar phase particles were utilized in the following cell experiments which was under the influence on particles phase hugely.

The physical and chemical properties were further identified by zeta potential, specific surface area (Fig. 3). Due to the similar synthetic route, the zeta potentials of both samples were close to each other and were around −14.8 mV. As for specific surface area, the Disso-HR and Multi-HS were around 14.29 $m^2\ g^{-1}$ and 19.80 $m^2\ g^{-1}$. The similar chemical–physical properties could eliminated extra disturbance elements.

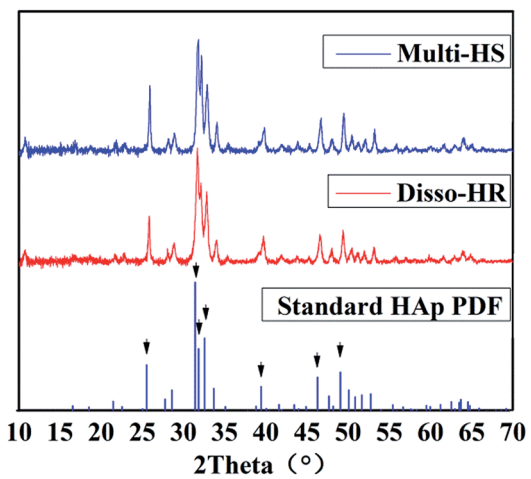

Fig. 2 XRD patterns of the particles. The black arrows represent the 7 intense characteristic peak namely (002) (211) (112) (300) (130) (222) (213).

3.2 Cell experiment

3.2.1 Cell proliferation and viability. mBMSCs co-cultured with materials for 1, 3, 5 days before reacting with CCK-8 assay. The results as shown in Fig. 4 revealed that mBMSCs cultured with Multi-HS were better proliferation compared with Disso-HR at 3 days and 5 days. Moreover the difference decreased with the incubating time increasing which was more obvious in cell viability Fig. 4. The cell viability calculating from CCK-8 kit assay showed the higher cell viability of mBMSCs when treated with Multi-HS. CCK-8 kit assay OD value version for cell proliferation was shown in ESI.†

3.2.2 Cytotoxicity of particles. L/D staining and LDH kit assay were operated to measure the cytotoxicity of the materials qualitatively and quantitatively. In L/D staining (Fig. 5A), the red spot representing dead cell was very rare especially in 48 and 72 h. However, in the time points of 24 h, rare green spot and red spot emerged which demonstrated the cytotoxicity expressed in early incubating time. Herein, LDH kit assay was utilized to measure the early cytotoxicity. From LDH kit assay in 3, 6, 12 h shown in Fig. 5B, the process of cytotoxicity were different. Disso-HR leaded to cytotoxicity at very early time (3 h) and the cytotoxicity remained stable from 3 to 12 hours, while the cytotoxicity of Multi-HS was half of that of Disso-HR and increasing with the time until reaching the close value of Disso-HR eventually. Since it was of crucial for following cellular behavior that cell adhere and expand at initial period. Although both particles show similar cytotoxicity when cultured for 12 h, the lower cytotoxicity at initial period (3 h and 6 h) can transfer to earlier cell proliferation.

3.2.3 Osteogenic differentiation of mBMSCs. After culturing 7 and 14 days in osteogenesis induced medium, the osteogenic expression (Fig. 6) were detected. OSX (osterix) were down-regulated than control, while the effect of Multi-HS on OSX were much more positive than that of Disso-HR. Tendency of ALP (alkaline phosphatase) was similar to OSX, namely down-regulated in both groups at early time then the difference decreased as the time prolonged to 14 days. What's more, the gene expression of Multi-HS group drew an even with blank control at 14 days after undergoing a huge contrast in early time. As for relative early osteogenic maker COL-I. Within the test duration, the 14 days-gene expression was up-regulation than that of 7 days, and expression of Multi-HS was twice as that of the Disso-HR. OPN (osteopontin) as an intermediate maker of osteogenesis, no significant variation in 14 days in our study revealed that the expression of OPN seemed active before 7 days, and the OPN expression of Multi-HS was twice as that of the others meaning that the differentiation from mesenchymal stem cells to mature stage osteoblasts happened earlier in Multi-HS group. Finally, the later marker OCN expressed low at 7 days while the expression up-regulation vigorously at 14 days. Overall, Multi-HS group presented earlier initiation and long duration to differentiation compared with Disso-HR.

3.2.4 ALP protein secretion. In Fig. 7, we investigated the protein secretion to supplement our gene expression results. Despite low expression in differentiation PCR results, the

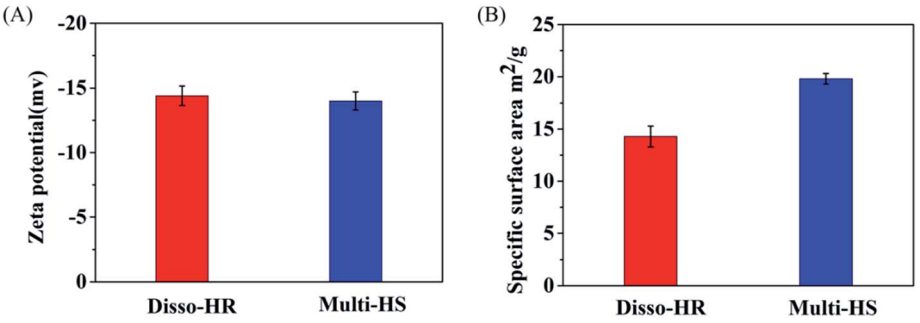

Fig. 3 Physical and chemical properties, (A) the zeta potential. (B) Specific surface area of Disso-HR and Multi-HS respectively.

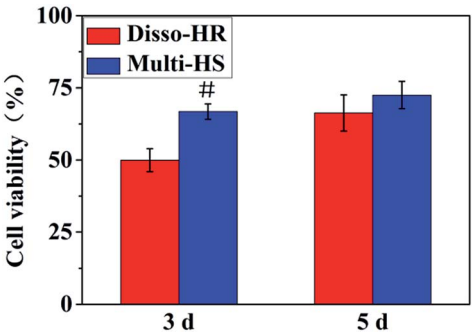

Fig. 4 Cell proliferation and viability: cell viability calculating according to the CCK-8 specification.

staining of ALP secretion was obvious in both groups. In the quantitative measurement, the secretion of Multi-HS expressed slightly higher than that of Disso-HR, while the tendency of both results were consistent.

3.2.5 The reciprocities of cell and particles. From SEM images (Fig. 8), we could see the interactions between materials and cells. In Fig. 8A1, there were many distinct cell filopodia intertwining micro-rods which could symbolized cellular phagocytosis. In Fig. 8A2, mBMSCs presented shuttle-shaped with clear focal adhesion, and micro-rods located on top cell membrane. Besides when the materials increased to a degree that every single cell exposed to too much miro-rods (Fig. 8A4), the cellular morphology shrinked which could be one way of cytotoxicity.

As for Multi-HS, we found, compared with upper cell surface, the bottom cell surface was endowed with better recognition and deform-ability to materials. From Fig. 8B1–B3, we can primarily observe that Multi-HS were too large to internalized by relative small mBMSCs. And mBMSCs were apt to contact with materials *via* bottom cell surface and deformed largely. From Fig. 8B4, when seeding cells to the pre-placed Multi-HS, mBMSCs still spreaded well and even tended to engulf some particles.

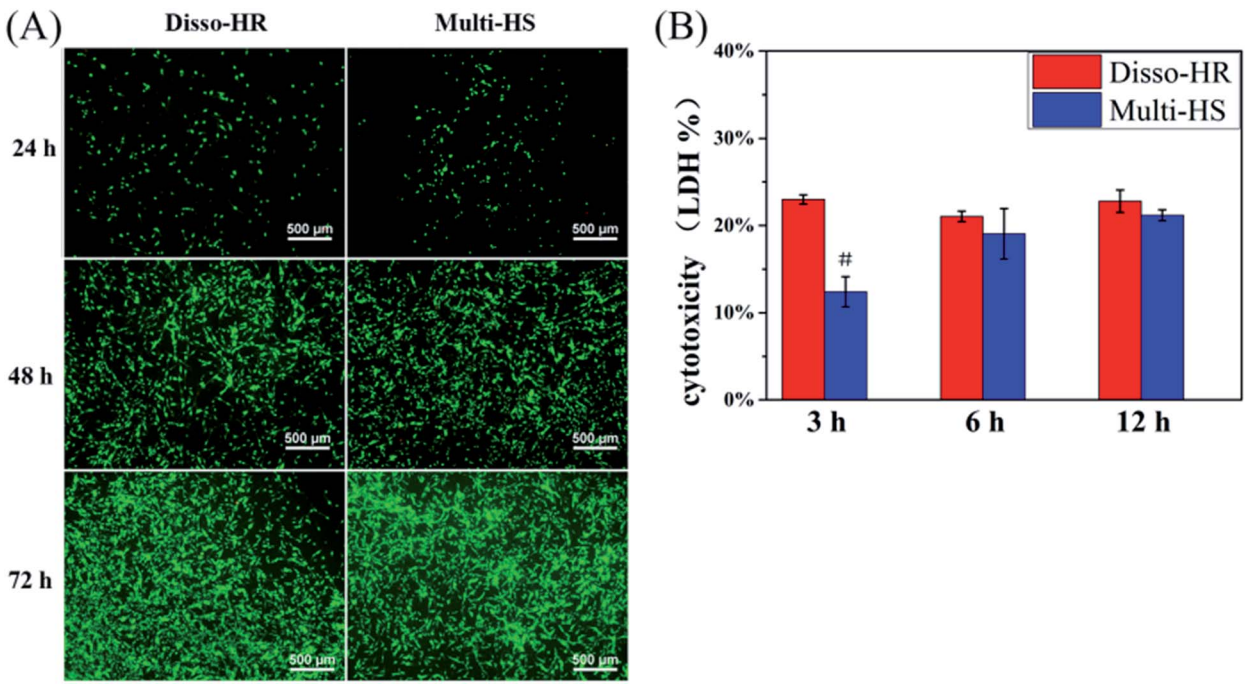

Fig. 5 Cytotoxicity: (A) live/dead staining. 24, 48 and 72 h set as test points; (B) LDH pierce kit. The early cytotoxicity were investigated.

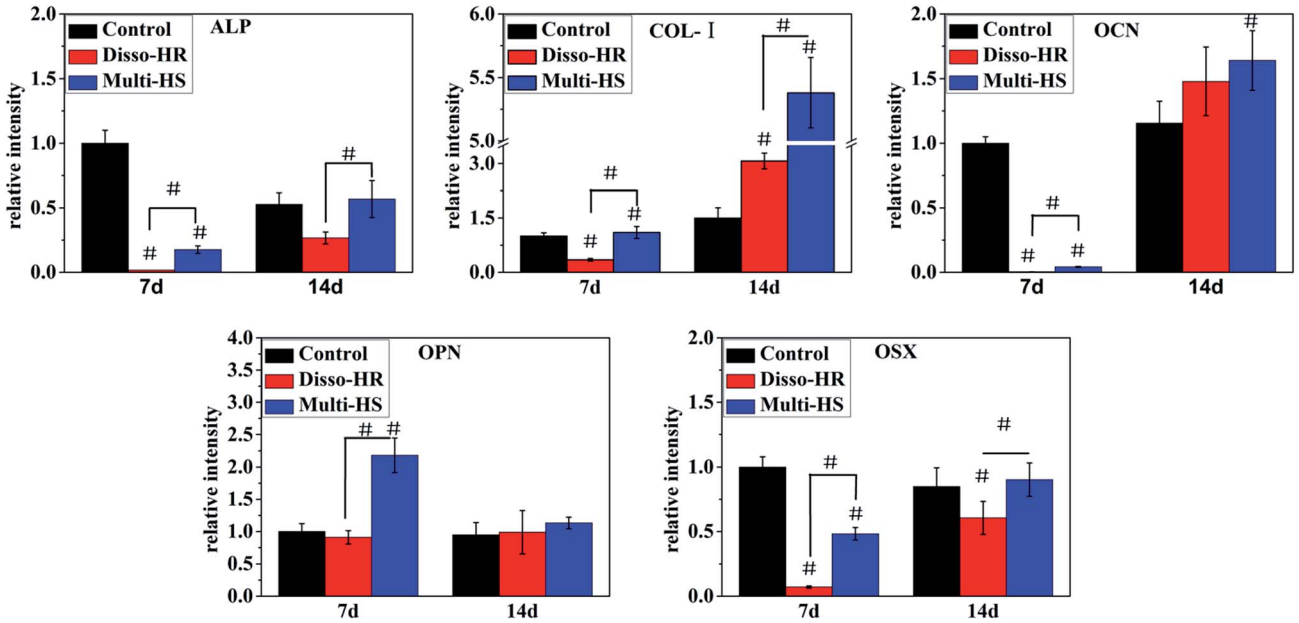

Fig. 6 Osteogenic differentiation real-time quantitative reverse transcription-polymerase chain reaction. The gene were alkaline phosphatase (ALP), collagen-I, osteocalcin (OCN), osteopontin (OPN), osterix (OSX) successively.

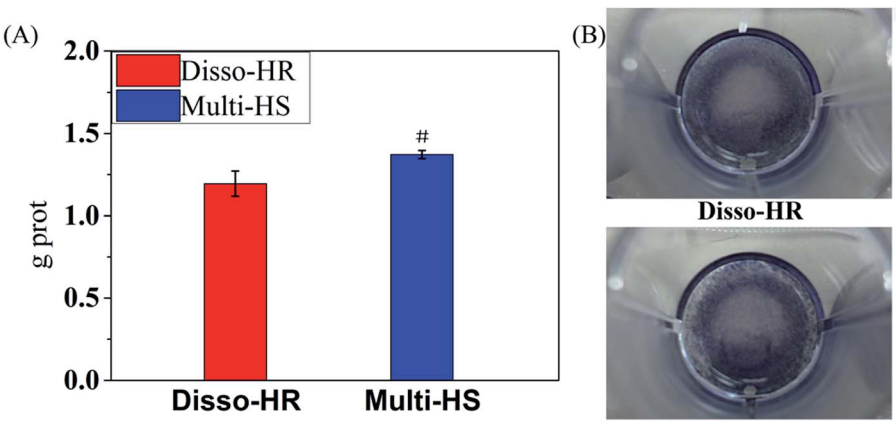

Fig. 7 ALP protein secretion. (A) Quantity measurement by ALP colorimetric kit, (B) BCIP/NBT staining.

4. Discussion

In the study, we designed a HAp hierarchical microsphere and dissociated rod synthesized in similar condition then investigated the effects of different micro-rods status on cellular behaviors. The characterization results indicated prepared uniform hierarchical structure microsphere (designated as Multi-HS) with sub-micro rods as the block unit whose shape were in analogy with uniform micro-rods (designated as Disso-HR). The two groups shared with similar XRD patterns and almost equal zeta potential. Besides, the specific surface area decrease radically and to a degree that close to each other by heat treatment under 700 °C for 3 hours.

Fig. 9 was a scheme of our cell experiments results to describe experiments in series. Firstly, very little red dots in L/D staining indicated low dead cells emerged and large-scale green dots in 48 hours could attribute to rapid mBMSCs proliferation after 24 hours. LDH activity shows the cytotoxicity of both were moderate. The above two experiments indicated the significant difference in cell proliferation was not caused by material-induced apoptosis. But the cytotoxicity process were different: Disso-HR remained the stable cytotoxicity while Multi-HS presented very low early cytotoxicity in 3 hours and increased to approach that of Disso-HR in following 12 hours. Owing to early cytotoxicity when was the key period for cell attachment and expansion, cell proliferation rate of Multi-HS group were higher and the cell viability undergone decreasing in Disso-HR group especially in 3 days viability of Disso-HR decreased 25% than that of Multi-HS. In osteogenic differentiation experiments, some concerned osteogenic gene were studied. OSX (osterix) were an important transcription factors for osteogenesis with zinc finger structure and regarded as the promoter gene in

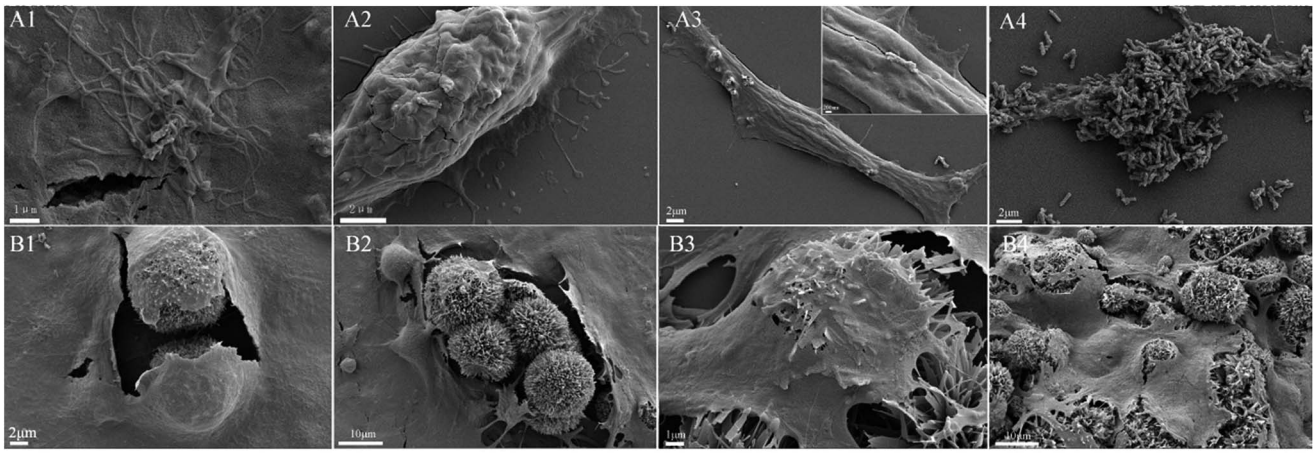

Fig. 8 SEM of cell–material interactions. (A) Disso-HR, (B) multi-HS (1) (2) (3) material–cell proportion ration 10 μg/1 × 10^4, seeding cells in advance, (4) proportion ration 100 μg/1 × 10^4, seeding materials in advance.

osteogenic differentiation.[24,25] ALP (alkaline phosphatase) as early osteogenic maker could serve as a plasma membrane for inorganic phosphates and regulate the phosphate metabolism through hydrolyzation of phosphate esters.[26] COL-I has been proved to a relative early osteogenic maker. It was recognized that collagen was the major protein composed the ECM (extracellular matrix) among which COL-I was the most important fibrillar type of collagen, and could serve as initial sites for inorganic mineral ions deposition.[27] OPN (osteopontin), it was considered as an intermediate maker of osteogenesis mainly expressed in early differentiation stage.[28] The OCN (osteocalcin) also known as bone gamma-carboxyglutamate protein (BGLAP) was a later maker of osteogenic differentiation, and acted on bone matrix deposition and mineralization.[29] From the results, we could see that the Multi-HS improved the cell differentiation and presented better osteo-conduction than Disso-HR in general. The side effects of Disso-HR may postpone the initial differentiation which could contribute to the cytotoxicity and down-regulation of cell viability in the prophase (see results in Fig. 5 and 6) while the gene expression of both groups in the long run were positive since the early lag phase was temporary. The osteogenic differentiation results were consistent with that

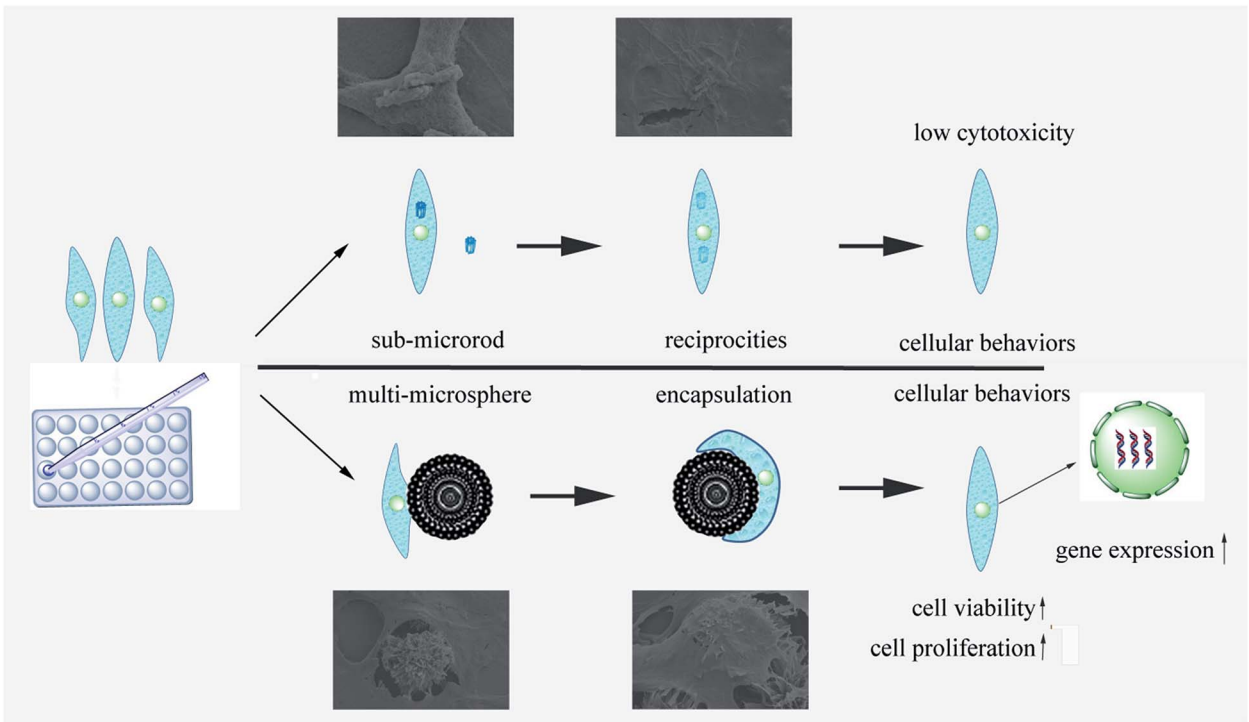

Fig. 9 Scheme for the process of cell–materials reciprocities.

of ALP protein secretion. In the SEM image, mBMSCs was a relative small cells and Multi-HS were too large to internized. Moreover too much local micro-rods to single cell leaded to cellular shrink. In fact, cellular intake went through endocytosis mediated by clathrin and alveole and reached ultimately lysosome to being digested. That endocytosis of dissociated rod might influence following cellular behaviours.[30–33] And mBMSCs were apt to contact with materials *via* bottom cell surface and deformed largely. When seeding cells to the preplaced Multi-HS, mBMSCs still spreaded well and tended to engulf some particles.

As a matter of facts, the multi-structured microsphere were more than just a research model but a potential "cell penetration cargo" delivery system.[34–36] Xie *et al.* synthesized nanowire with Al_2O_3 surface membrane to penetrate cell and delivery cargoes like small interfere RNA. What's more, a large flat form was indispensable for the nanowire or string so our multi-structured microsphere with spiky block unit on the surface could be an excellent candidate. Hydroxyapatite possess excellent bioactivity and biocompatibility than bio-inert Al_2O_3 so that cell would internalize our HA spiky block unit rather than to penetrate cells then accomplish intracellular delivery and transfection meanwhile produce less cytotoxicity. However, our weak-point were also obvious. From protein adsorption results (see ESI†), our materials especially the microsphere didn't absorb much cargoes including lysozyme and RNA is negative in analogy with lysozyme. Surface modification need to decorate HA surface.

5. Conclusion

In our work, *via* similar reaction system and procedure we synthesized uniform hierarchical structure microsphere with sub-micro rods as the block unit and sub-micro rods HAp. Compare the effects of different micro-rods status on cellular behavior. We found out that particles wouldn't cause apoptosis directly. In fact, HAp particles cause low cytotoxicity while cell viability decreased leading to different cellular proliferation and differentiation. The process could describe as: endocytosis of dissociated rod lead to down-regulation in cell viability whose decline generated the influence of following behaviours. From the groups comparison, dissociated micro-rods property were inferior to that of micro-rods that located on big platform. The results verified the wear particles from implant scaffolds leading to implant failure and may explain why many rods located on natural bone surface yet wouldn't cause side effect. Besides, through proper modification on surface, our Multi-HS could be an excellent candidate for cell penetration intracellular delivery system.

Acknowledgements

This work was financially supported by the National Basic Research Programme of China (Grant No. 2012CB619100), the National Natural Science Foundation of China (Grant No. 51232002), the Science and Technology Programme of Guangzhou city(Grant No. 201607010234), the Fundamental Research Funds for the Central Universities (Grant No. 2015ZZ009), Guangdong Natural Science Funds for Distinguished Young Scholar (Grant No. 2016A030306018) and China Postdoctoral Science Foundation(Grant No. 2016M592487).

References

1 R. Z. LeGeros, *Chem. Rev.*, 2008, **108**, 4742–4753.
2 E. Landi, G. Celotti, G. Logroscino and A. Tampieri, *J. Eur. Ceram. Soc.*, 2003, **23**, 2931–2937.
3 K. J. L. Burg, S. Porter and J. F. Kellam, *Biomaterials*, 2000, **21**, 2347–2359.
4 X.-Y. Zhao, Y.-J. Zhu, F. Chen, B.-Q. Lu, C. Qi, J. Zhao and J. Wu, *CrystEngComm*, 2013, **15**, 7926.
5 X.-Y. Zhao, Y.-J. Zhu, B.-Q. Lu, F. Chen, C. Qi, J. Zhao and J. Wu, *Mater. Res. Bull.*, 2014, **55**, 67–70.
6 M. Huang and Y. Wang, *J. Mater. Chem.*, 2012, **22**, 626–630.
7 M. Ni and B. D. Ratner, *Biomaterials*, 2003, **24**, 4323–4331.
8 H. Ehrlich, B. Krajewska, T. Hanke, R. Born, S. Heinemann, C. Knieb and H. Worch, *J. Membr. Sci.*, 2006, **273**, 124–128.
9 H. Wang, Y. Li, Y. Zuo, J. Li, S. Ma and L. Cheng, *Biomaterials*, 2007, **28**, 3338–3348.
10 V. V. Sokolova, I. Radtke, R. Heumann and M. Epple, *Biomaterials*, 2006, **27**, 3147–3153.
11 M. Jordan and F. Wurm, *Methods*, 2004, **33**, 136–143.
12 Y. Huang, G. Zhou, L. Zheng, H. Liu, X. Niu and Y. Fan, *Nanoscale*, 2012, **4**, 2484–2490.
13 Y. Cai, Y. Liu, W. Yan, Q. Hu, J. Tao, M. Zhang, Z. Shi and R. Tang, *J. Mater. Chem.*, 2007, **17**, 3780.
14 S. B. Goodman, T. Ma, R. Chiu, R. Ramachandran and R. Lane Smith, *Biomaterials*, 2006, **27**, 6096–6101.
15 M. Motskin, D. M. Wright, K. Muller, N. Kyle, T. G. Gard, A. E. Porter and J. N. Skepper, *Biomaterials*, 2009, **30**, 3307–3317.
16 P. Laquerriere, A. Grandjean-Laquerriere, E. Jallot, G. Balossier, P. Frayssinet and M. Guenounou, *Biomaterials*, 2003, **24**, 2739–2747.
17 Y. Hong, H. Fan, B. Li, B. Guo, M. Liu and X. Zhang, *Mater. Sci. Eng., R*, 2010, **70**, 225–242.
18 H. Yang, L. Hao, N. Zhao, C. Du and Y. Wang, *CrystEngComm*, 2013, **15**, 5760–5763.
19 H. Yang, H. Zeng, L. Hao, N. Zhao, C. Du, H. Liao and Y. Wang, *J. Mater. Chem. B*, 2014, **2**, 4703.
20 H. Yang, L. Hao, C. Du and Y. Wang, *RSC Adv.*, 2013, **3**, 23184.
21 H. Yang, L. Hao, N. Zhao, M. Huang, C. Du and Y. Wang, *Mater. Chem. Phys.*, 2013, **141**, 488–494.
22 L. Hao, H. Yang, N. Zhao, C. Du and Y. Wang, *Powder Technol.*, 2014, **253**, 172–177.
23 H. Duan, Y. Ma, X. Liu, L. Hao and N. Zhao, *RSC Adv.*, 2015, **5**, 83522–83529.
24 T. Koga, Y. Matsui, M. Asagiri, T. Kodama, B. de Crombrugghe, K. Nakashima and H. Takayanagi, *Nat. Med.*, 2005, **11**, 880–885.
25 Y. Nishio, Y. Dong, M. Paris, R. J. O'Keefe, E. M. Schwarz and H. Drissi, *Gene*, 2006, **372**, 62–70.

26 L. Xia, Z. Zhang, L. Chen, W. Zhang, D. Zeng, X. Zhang, J. Chang and X. Jiang, *Eur. Cells Mater.*, 2011, **22**, e82.
27 N. Wang, H. Li, W. Lü, J. Li, J. Wang, Z. Zhang and Y. Liu, *Biomaterials*, 2011, **32**, 6900–6911.
28 F. P. Reinholt, K. Hultenby, A. Oldberg and D. Heinegård, *Proc. Natl. Acad. Sci. U. S. A.*, 1990, **87**, 4473–4475.
29 N. K. Lee, H. Sowa, E. Hinoi, M. Ferron, J. D. Ahn, C. Confavreux, R. Dacquin, P. J. Mee, M. D. McKee and D. Y. Jung, *Cell*, 2007, **130**, 456–469.
30 Z. Chen, Z. Li, Y. Lin, M. Yin, J. Ren and X. Qu, *Biomaterials*, 2013, **34**, 1364–1371.
31 Y. Wang and H. Gu, *Adv. Mater.*, 2015, **27**, 576–585.
32 P. Kesharwani, V. Gajbhiye and N. K. Jain, *Biomaterials*, 2012, **33**, 7138–7150.
33 L. Y. T. Chou, K. Ming and W. C. W. Chan, *Chem. Soc. Rev.*, 2011, **40**, 233–245.
34 A. K. Shalek, J. T. Robinson, E. S. Karp, J. S. Lee, D. R. Ahn, M. H. Yoon, A. Sutton, M. Jorgolli, R. S. Gertner, T. S. Gujral, G. MacBeath, E. G. Yang and H. Park, *Proc. Natl. Acad. Sci. U. S. A.*, 2010, **107**, 1870–1875.
35 X. Xie, A. M. Xu, M. R. Angle, N. Tayebi, P. Verma and N. A. Melosh, *Nano Lett.*, 2013, **13**, 6002–6008.
36 X. Xie, A. M. Xu, S. Leal-Ortiz, Y. H. Cao, C. C. Garner and N. A. Melosh, *ACS Nano*, 2013, **7**, 4351–4358.